A ZVZCS PWM FB DC/DC Converter Using a Modified Energy-Recovery Snubber

Eun-Soo Kim, *Member, IEEE*, and Yoon-Ho Kim, *Senior Member, IEEE*

***Abstract*—The conventional high-frequency phase-shifted zero-voltage-switching (ZVS) full-bridge dc/dc converter has a disadvantage, in that a circulating current flows through transformer and switching devices during the freewheeling interval. Due to this circulating current, rms current stress, conduction losses of the transformer and switching devices are increased. To alleviate this problem, this paper proposes an improved zero-voltage zero-current switching (ZVZCS) phase-shifted full-bridge (FB) dc/dc converter with a modified energy-recovery snubber (ERS) attached at the secondary side of transformer. Also, the small signal model of the proposed ZVZCS FB dc/dc converter is derived by incorporating the effects introduced by a transformer leakage inductance and an ERS to achieve ZVZCS. Both analysis and experiment are performed to verify the proposed topology by implementing a 7-kW (120 Vdc, 58 A) 30-kHz insulated-gate-bipolar-transistor-based experimental circuit**

***Index Terms*—Energy-recovery snubber, full-bridge (FB) dc/dc converter, small-signal modeling, zero-voltage switching (ZVS), zero-voltage zero-current switching (ZVZCS).**

I. Introduction

RECENTLY, the phase-shifted full-bridge (FB) dc/dc converter has been proposed to reduce the component stress of voltage and current and the switching losses in the traditional pulsewidth-modulated (PWM) converter. However, because of the phase-shifted PWM control, the converter has a disadvantage, in that a circulating current, which is the sum of the reflected output current (nI_o) and transformer primary magnetizing current (I_m), flows through the transformer and switching devices during the freewheeling interval (t_1-t_3, t_6-t_8 as shown in Fig. 1(b). Due to the circulating current, rms current stresses of transformer and switching devices are still high compared to those of the conventional hard-switching PWM full-bridge converter. To alleviate these problems, zero-voltage zero-current switching (ZVZCS) FB dc/dc converters using a simple auxiliary circuit have been presented [1]–[3]. However, the use of the simple auxiliary circuits to reduce the circulating current has disadvantages such as overvoltage and severe parasitic ringing in the secondary side of the transformer. This paper proposes an improved ZVZCS phase-shifted FB dc/dc converter using the modified energy-recovery snubber (ERS) attached at the secondary side of the transformer. By using the modified ERS, the proposed converter can reduce the circulating current flowing through switching devices during the freewheeling interval and voltage stress in the secondary rectifier diodes. Also in this paper, the small-signal model of the ZVZCS FB dc/dc converter is derived by incorporating the effects introduced by the transformer leakage inductance and by the use of the ERS to achieve ZVZCS. The corresponding transfer functions of the ZVS FB dc/dc converter and ZVZCS FB dc/dc converter are presented to show a significant difference between them. Both

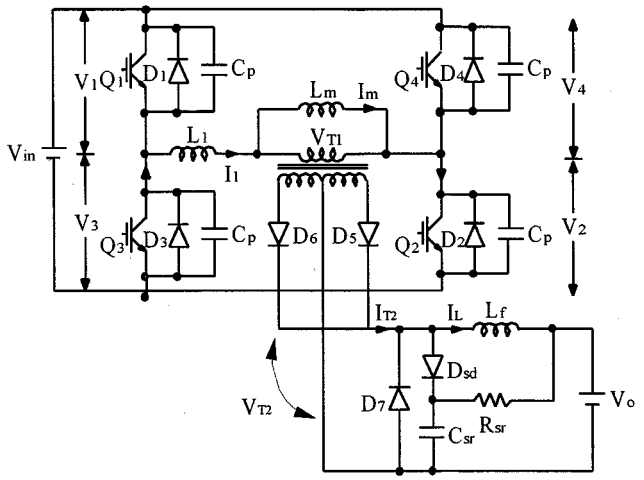

(a)

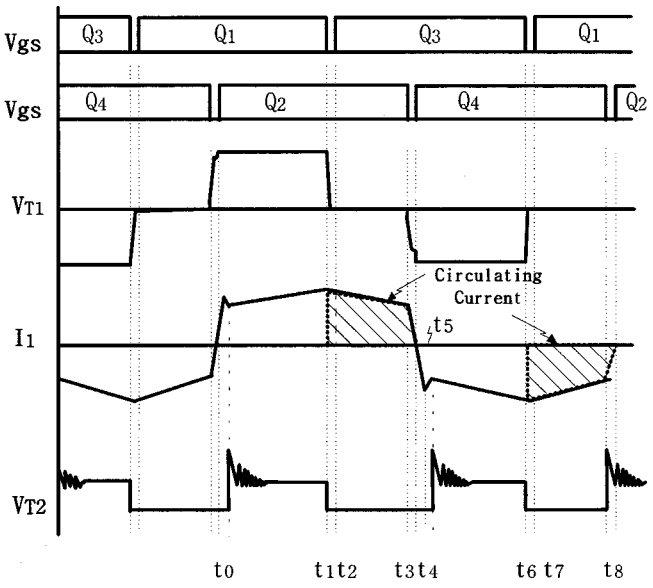

(b)

Fig. 1. Phase-shifted ZVS FB dc/dc converter and its waveforms. (a) Conventional ZVS FB dc/dc converter. (b) Operation waveforms.

Manuscript received November 28, 2000; revised June 14, 2002. Abstract published on the Internet July 15, 2002.

E.-S. Kim is with the Department of Electrical and Electronic Engineering, Jeonju University, Jeonju 560-759, Korea (e-mail: eskim@jeonju.ac.kr).

Y.-H. Kim is with the Department of Electrical Engineering, Chung-Ang University, Seoul 156-756, Korea (e-mail: yhkim@cau.ac.kr).

Publisher Item Identifier 10.1109/TIE.2002.803237.

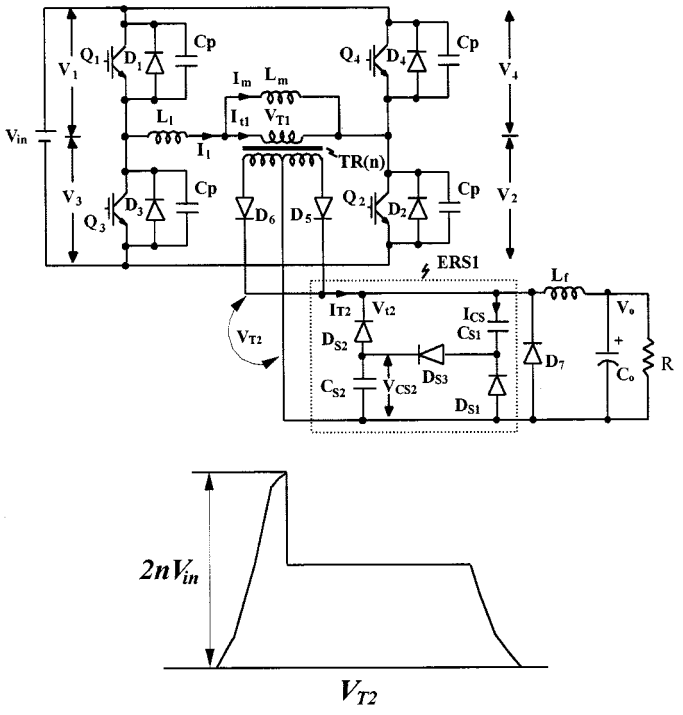

Fig. 2. ZVZCS FB dc/dc converter using ERS1 and voltage waveform across D_7.

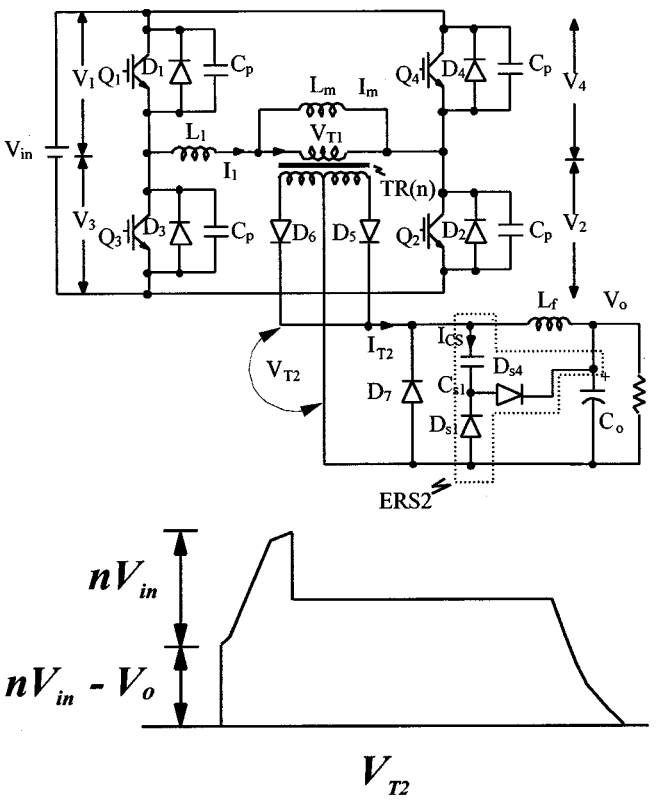

Fig. 3. ZVZCS FB dc/dc converter using the simplified ERS2 and voltage waveform across D_7.

analysis and experiment are performed to verify the proposed topology by implementing a 7-kW (120 Vdc, 58 A) 30-kHz insilated-gate-bipolar-transistor (IGBT)-based experimental circuit.

II. ZVZCS FB DC/DC Converters Using the ERS

By using the ERS (ERS1) instead of adding a tapped inductor and a saturable reactor to reduce rms current stress such as described in the references [1], [2], the converter can reduce the circulating current flowing during the freewheeling interval. As shown in Fig. 2, the energy stored in the snubber capacitors (C_{s1}, C_{s2}) during conduction interval starts discharging when the transformer secondary voltage in the freewheeling interval becomes zero. Due to the discharging of the snubber capacitors (C_{s1}, C_{s2}), both primary and secondary currents of the transformer become zero. Therefore, the rectifier diodes D_5 and D_6 are biased in reverse and the secondary windings of the transformer are opened. Thus, the rms currents for the transformer and switches are considerably reduced in the freewheeling interval. Also, the converter achieves ZVS for secondary rectifier diodes (D_5, D_6) and freewheeling diode (D_7) because the ERS (ERS1) at the turn-on time of switches (Q_1, Q_2 and Q_3, Q_4) provides a low-impedance path through the transformer, a snubber capacitor (C_{s1}), a snubber diode (D_{s3}), and a snubber capacitor (C_{s2}). However, in this case, during the transition from off stage to active stage, the serial resonance circuit is formed with leakage inductance of the transformer and snubber capacitors of the secondary and the secondary current (I_{T1}/n) begins to flow to C_{s1}, D_{s3}, and C_{s2} through the transformer and rectifier diodes. During the charging process, snubber capacitors (C_{s1}, C_{s2}) are charged up to the secondary voltage ($nV_{\rm in}$) of the transformer, respectively

$$V_{T2}(t) = V_{cs1}(t) + V_{cs2}(t) = nV_{\rm in} \cdot \left[1 - \cos\sqrt{\frac{2}{n^2 L_l C_s}} \cdot t\right] \quad (1)$$

$$V_{T2\rm peak} = 2nV_{\rm in} \quad (2)$$

where $C_{s1} = C_{s2} = C_s$, $n = N_s/N_p$..

As a result, overvoltage occurs on the secondary of the transformer. Due to the relatively high impedance of the resonant tank, the snubbing or clamping effect for the secondary transient voltage is also lost. As shown in Fig. 3, the simplified ERS (ERS2) can be used to reduce the circulating current and clamp the secondary transient voltage [3]. However, this snubber circuit cannot achieve ZVS in the secondary side of the FB dc/dc converter because the serial resonance circuit is formed with transformer leakage inductance L_l, snubber capacitor C_{s1}, snubber diode D_{s4}, and output capacitor C_o

$$V_{T2}(t) = V_o + (nV_{\rm in} - V_o) \cdot \frac{C_o}{C_{s1} + C_o}\left[1 - \cos\sqrt{\frac{C_{s1} + C_o}{n^2 L_l C_{s1} C_o}} \cdot t\right] \quad (3)$$

$$V_{T2\rm peak} = 2nV_{\rm in} - V_o. \quad (4)$$

Also, the voltage source to reset the primary leakage current in the FB dc/dc converter using the simplified ERS (ERS2) is only the discharge voltage (V_{cs}) of snubber capacitor C_{s1}. Therefore, the ZVZCS condition cannot be expanded to the heavy load.

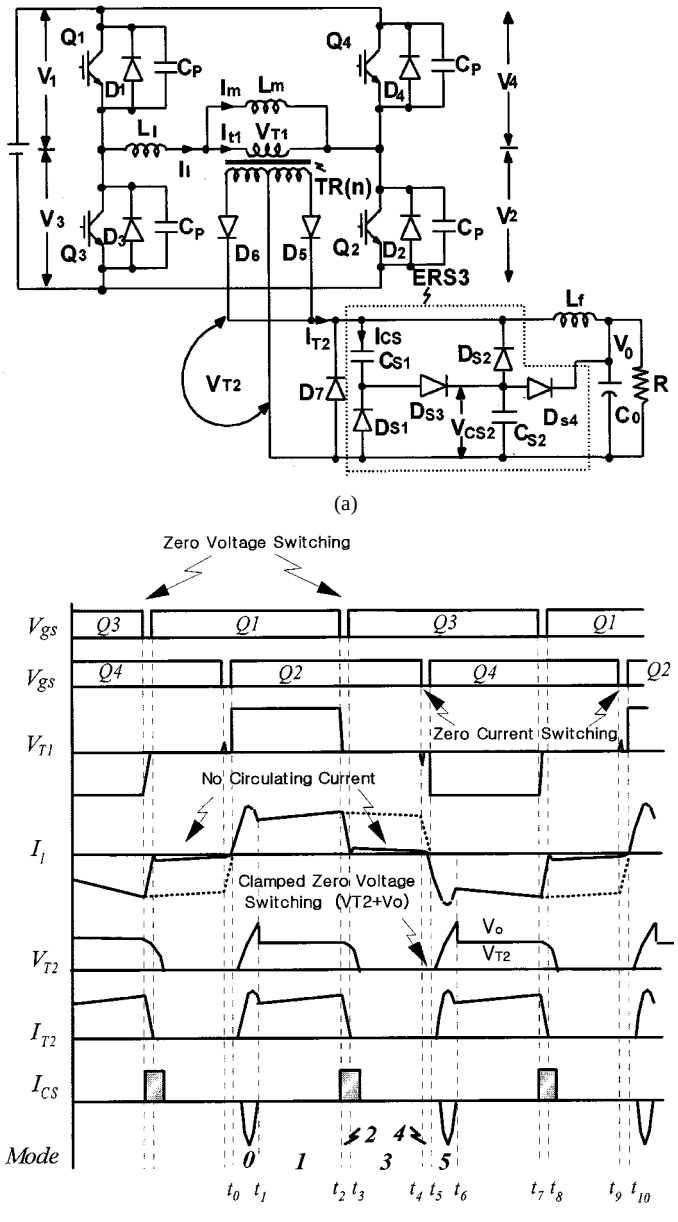

Fig. 4. Proposed ZVZCS FB dc/dc converter using the modified clamp circuit ERS3. (a) ZVZCS FB dc/dc converter using the modified energy-recovery snubber ERS3. (b) Operation waveforms.

III. Proposed ZVZCS FB DC/DC Converter Using a Modified ERS

Fig. 4 shows the proposed phase-shifted ZVZCS FB dc/dc converter that applies the modified ERS (ERS3) to minimize the circulating current and the secondary transient overvoltage. The modified ERS (ERS3) that consists of four fast-recovery diodes (D_{s1}–D_{s4}) and two resonant capacitors (C_{s1}, C_{s2}) is inserted between the transformer secondary-side rectifier (D_5, D_6) and output inductor (L_f) to reduce the circulating current. The operating mechanism and circuit configuration of the proposed circuit are similar to the ZVZCS FB dc/dc converter using the ERS (ERS1) except for inserting the snubber diode (D_{s4}). Snubber diode D_{s4} is connected in the output capacitor C_o in order to clamp the snubber capacitor voltage V_{cs2} from the secondary voltage ($nV_{\rm in}$) to the output voltage (V_o)

$$V_{T2\rm peak} = nV_{\rm in} + V_o. \tag{5}$$

Here, due to discharging of the energy stored in the snubber capacitors (C_{s1}, C_{s2}) during the conduction interval ($t_0 - t_2$, $t_5 - t_7$), both primary and secondary circulating current through the transformer become zero during the freewheeling interval ($t_2 - t_4$, $t_7 - t_9$) if the discharge time T_{cs} of the energy stored in the snubber capacitors (C_{s1}, C_{s2}) is satisfied by the following (7):

$$T_{cs} \approx V_{cs} \cdot \frac{(C_{s1} + C_{s2})}{I_o} > T_{L1} \approx \frac{n^2 L_l \cdot I_L}{V_{cs}(0)} \tag{6}$$

$$C_s > \frac{1}{2} \cdot \frac{n^2 L_l \cdot I_L^2}{V_{cs}(0)^2} \tag{7}$$

where $C_{s1} = C_{s2} = C_s$ and $n^2 L_l = n^2 L_{l1} + L_{l2}$.

Then, the rectifier diodes D_5 and D_6 are biased in reverse and the secondary windings of the transformer are opened. Due to the reduced circulating current, the conduction losses are minimized in switches and transformer during the freewheeling interval ($t_2 - t_4$, $t_7 - t_9$). Therefore, the proposed ZVZCS FB dc/dc converter can reduce the secondary transient overvoltage as well as the circulating current. Also, the modified ERS adopted in this study recovers the transformer leakage energy and switching losses to the load.

IV. Small-Signal Characteristics of ZVZCS FB DC/DC Converter

The small-signal model of the ZVS FB dc/dc converter can be derived from the averaged small-signal model of the PWM buck converter with incorporating additional effect of the transformer leakage inductance [4]. It can be seen from the description of the circuit operation that the effective duty cycle ($d_{\rm eff} = D_{\rm eff} + \hat{d}_{\rm eff}$) of the transformer secondary voltage depends on not only the duty cycle (d) of the primary voltage, but also the output filter inductor current i_L, the leakage inductance L_l, the input voltage $V_{\rm in}$, and the switching frequency f_s. Also, the small-signal model of the ZVZCS FB dc/dc converter can be expanded from the averaged small-signal model of the ZVS FB dc/dc converter by incorporating the use of the ERS (ERS3 or ERS1) as shown in Fig. 5. Because of the presence of the ERS (ERS3 or ERS1), small-signal characteristics of the proposed ZVZCS FB dc/dc converter are different from the corresponding characteristics of the conventional ZVS FB dc/dc converter. To accurately model the dynamic behavior of the ZVZCS FB dc/dc converter, it is necessary to know the contributions of the leakage inductance L_l and the energy-recovery snubber, f_s, $\hat{i}_{Lf}$, $\hat{v}_{\rm in}$, and $\hat{d}$, $\hat{d}_{\rm eff}$ where the magnetizing current I_m is assumed to be constant and negligibly small compared with the primary current I_{T1} and the inductor current i_L.

Delay Interval d_1: When the switches Q_1, Q_2 are conducting, the input voltage is applied to the transformer leakage inductance L_l and the reflected primary current I_{T2} increases until it reaches the inductor current i_L. While the secondary

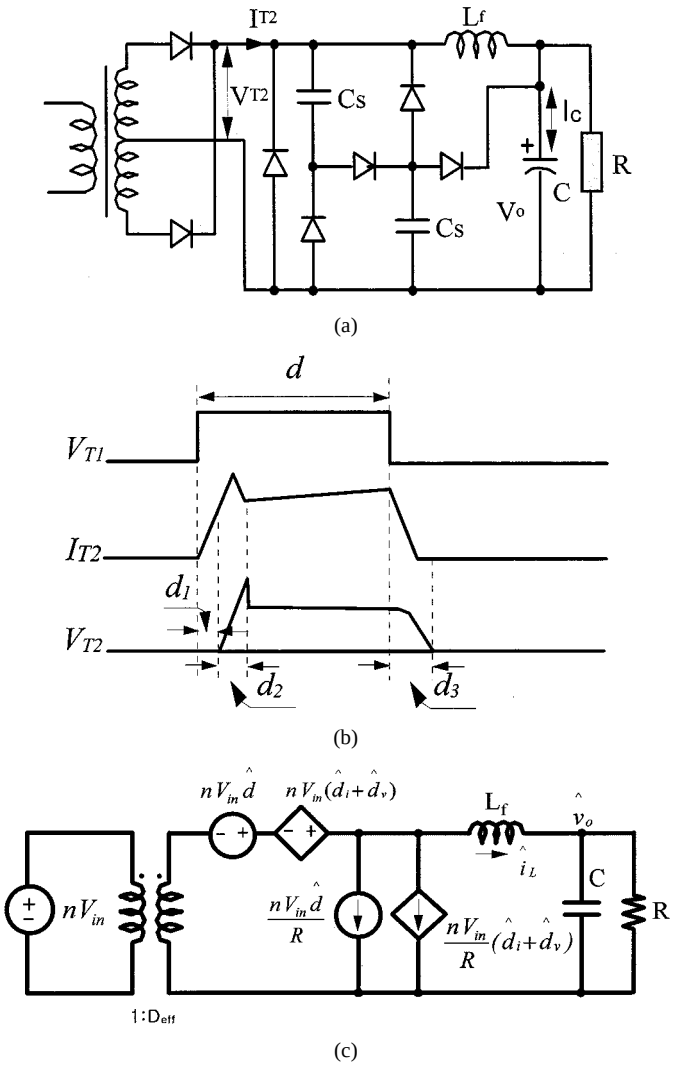

Fig. 5. Secondary circuit waveforms and small-signal model of FB dc/dc converter (a) Secondary circuit using the modified snuber ERS3. (b) Operating waveforms. (c) Small-signal circuit model of FB dc/dc converter.

voltage nV_{in} due to the inductor current i_L increases, the additional delay d_1 can be produced as follows:

$$\Delta t_1 = \frac{n^2 L_l}{nv_{\text{in}}} i_L, d_1 = -\frac{\Delta t_1}{\frac{T_s}{2}} = -\frac{2n^2 L_l f_s}{nv_{\text{in}}} i_L. \tag{8}$$

Delay Interval d_2: By using the ERS (ERS3 or ERS1) in the ZVZCS FB dc/dc converter, the serial resonance circuit is formed with leakage inductance L_l of the transformer and snubber capacitors (C_{s1}, C_{s2}) of the secondary and the secondary current (I_{T1}/n) begins to flow to C_{s1}, D_{s3}, and C_{s2} through the transformer and rectifier diodes. Therefore, the additional delay d_2 in the charging process can be calculated as follows:

$$d_2 = -\frac{\Delta t_2}{\frac{T_s}{2}} = -\frac{\sqrt{\frac{n^2 L_l C_s}{2}} \cdot \pi}{\frac{T_s}{2}} = -\sqrt{2n^2 L_l C_S} \cdot \pi \cdot f_s \tag{9}$$

where $n^2 L_l$ is the reflected leakage inductance to the secondary of transformer.

Delay Interval d_3: When snubber capacitors (C_{s1}, C_{s2}) start discharging during the freewheeling interval, the total capacity and capacitance of the snubber capacitors doubles. Due to the discharging of the snubber capacitors (C_{s1}, C_{s2}), both primary and secondary currents of the transformer become zero and then the rectifier diodes D_5 and D_6 are biased in reverse and the secondary windings of the transformer are opened. Thus, the secondary voltage V_{T2} decreases until it reaches zero

$$\Delta t_3 = \frac{2nC_s nv_{\text{in}}}{i_L} \tag{10}$$

$$d_3 = \frac{\frac{2nC_s nv_{\text{in}}}{i_L}}{\frac{T_s}{2}} = \frac{4nC_s f_s nv_{\text{in}}}{i_L}. \tag{11}$$

Here, the effective duty ratio is obtained as follows:

$$\begin{aligned} d_{\text{eff}} &= d + d_1 + \frac{d_2}{2} + \frac{d_3}{2} \\ &= d - \frac{2n^2 L_l f_s}{nv_{\text{in}}} i_L \\ &\quad - \frac{\left(\sqrt{2n^2 L_l C_s} \cdot \pi \cdot f_s\right)}{2} + \frac{4nC_s f_s nv_{\text{in}}}{2 \cdot i_L} \\ &= d + \frac{T_1}{nv_{\text{in}}} i_L + T_2 + \frac{T_3}{i_L} nv_{\text{in}} \end{aligned} \tag{12}$$

where $T_1 = -2n^2 L_l f_s$, $T_2 = -\sqrt{n^2 L_l C_s/2} \cdot \pi \cdot f_s$, $T_3 = 2nC_s f_s$.

By introducing perturbations to the effective duty ratio of (12) as

$$d_{\text{eff}} = D_{\text{eff}} + \hat{d}_{\text{eff}} \quad d = D + \hat{d} \tag{13}$$

$$nv_{\text{in}} = nV_{\text{in}} + n\hat{v}_{\text{in}} \quad i_L = I_L + \hat{i}_L. \tag{14}$$

The small-signal equation is obtained as

$$D_{\text{eff}} + \hat{d}_{\text{eff}} = D + \hat{d} + \frac{T_1(I_L + \hat{i}_L)}{nV_{\text{in}} + n\hat{v}_{\text{in}}} + T_2 + \frac{T_3(nV_{\text{in}} + n\hat{v}_{\text{in}})}{I_L + \hat{i}_L}. \tag{15}$$

By neglecting of the terms of dc and high order, the simplified small-signal equation is obtained as follows:

$$\begin{aligned} \hat{d}_{\text{eff}} &= \hat{d} + \left[\frac{D - D_{\text{eff}} + T_2}{I_L} + \frac{2T_1}{nV_{\text{in}}}\right] \hat{i}_L \\ &\quad + \left[\frac{D - D_{\text{eff}} + T_2}{nV_{\text{in}}} + \frac{2T_3}{I_L}\right] n\hat{v}_{\text{in}} \\ &= \hat{d} + \hat{d}_i + \hat{d}_v \end{aligned} \tag{16}$$

where

$$\hat{d}_i = \left[\frac{D - D_{\text{eff}} + T_2}{I_L} + \frac{2T_1}{nV_{\text{in}}}\right] \hat{i}_L$$

$$\hat{d}_v = \left[\frac{D - D_{\text{eff}} + T_2}{nV_{\text{in}}} + \frac{2T_3}{I_L}\right] n\hat{v}_{\text{in}}.$$

The first term in (16) represents a change in the effective duty cycle d_{eff} due to the perturbation in the primary duty cycle. The second term represents the change of d_{eff} caused by the perturbation of the output filter inductor current. The third term represents the change of d_{eff} caused by the perturbation of input voltage. The small-signal model to derive the transfer functions of the ZVS and ZVZCS FB dc/dc converter is shown in Fig. 5(c). The contribution of $\hat{d}_i$ and $\hat{d}_v$ is represented by two controlled

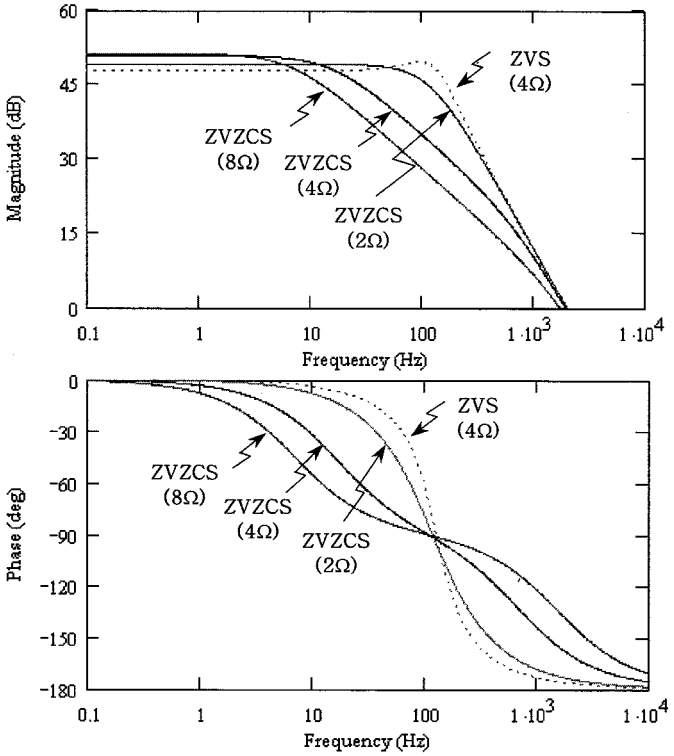

Fig. 6. Simulation results of the control-to-output voltage transfer function in the proposed ZVZCS FB dc/dc converter and the conventional ZVS FB dc/dc converter.

sources. From Fig. 5(c), the control-to-output voltage transfer function is given by

$$G_{ZVS}(s) = \frac{\hat{v_o}}{\hat{d}} = H_o n V_{\text{in}} \frac{Z_f}{Z_f + R_d} \tag{17}$$

where

$$\begin{aligned} R_d &= -4n^2 L_l f_s \\ Z_f &= \frac{(RL_f C s^2 + L_f s + R)}{(RC's + 1)} \\ H_o &= \frac{1}{(L_f C s^2 + \frac{L_f}{R} s + 1)} \end{aligned}$$

Z_f: output impedance; H_o: transfer function of output filter;

$$\begin{aligned} G_{ZVZCS}(s) &= \frac{\hat{v_o}}{\hat{d}} = H_o n V_{\text{in}} \frac{Z_f}{Z_f + R_{ZVZCS}} \\ &= \frac{n V_{\text{in}} \omega_o^2}{s^2 + s\left(\frac{L_f}{RC} + \frac{R_{ZVZCS}}{L_f}\right) + \omega_o^2 \left(1 + \frac{R_{ZVZCS}}{R}\right)} \\ &= \frac{n V_{\text{in}} \omega_0^2}{s^2 + 2\omega_0 \zeta s + \omega_0^2 \left(1 + \frac{R_{ZVZCS}}{R}\right)} \end{aligned} \tag{18}$$

where

$$\begin{aligned} R_{ZVZCS} &= -nV_{\text{in}} \cdot \left[\frac{(D - D_{\text{eff}} + T_2)}{I_L} + \frac{2T_1}{nV_{\text{in}}}\right] \\ \omega_o &= \sqrt{1/L_f C} \\ \zeta &= \frac{1}{2R}\sqrt{\frac{L_f}{C}} + \frac{R_{ZVZCS}}{2}\sqrt{\frac{C}{L_f}}. \end{aligned}$$

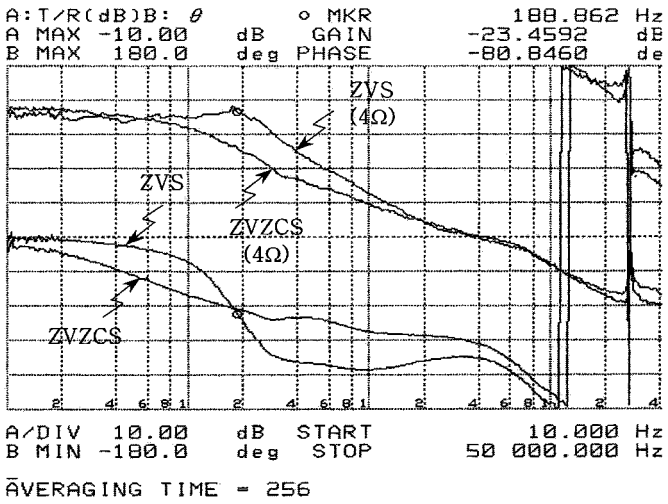

Fig. 7. Measurement results of the control-to-output voltage transfer function in ZVS and ZVZCS converter (output voltage: 120 Vdc, R : 4Ω).

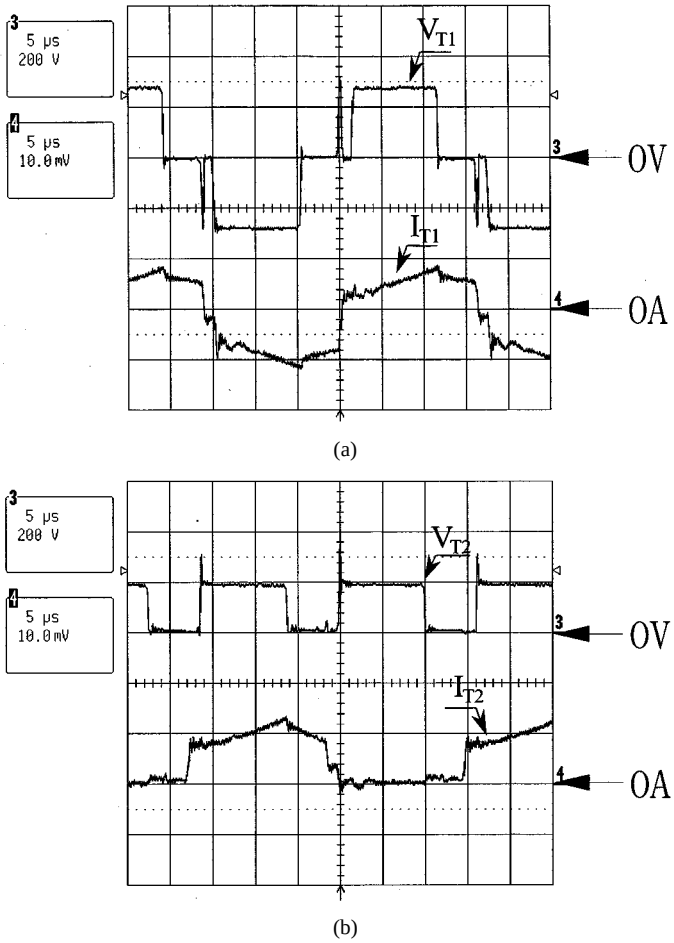

Fig. 8. Waveforms of the conventional ZVS FB dc/dc converter with *RCD* snubber (200 V/div, 50 A/div, 5 μs/div). (a) Voltage and current waveforms of the primary. (b) Voltage and current waveforms of the secondary.

Equations (17) and (18) are the control-to-output voltage transfer functions of the conventional ZVS FB dc/dc converter and the proposed ZVZCS FB dc/dc converter, respectively. The first term of ζ shown in (18) is the damping in the buck

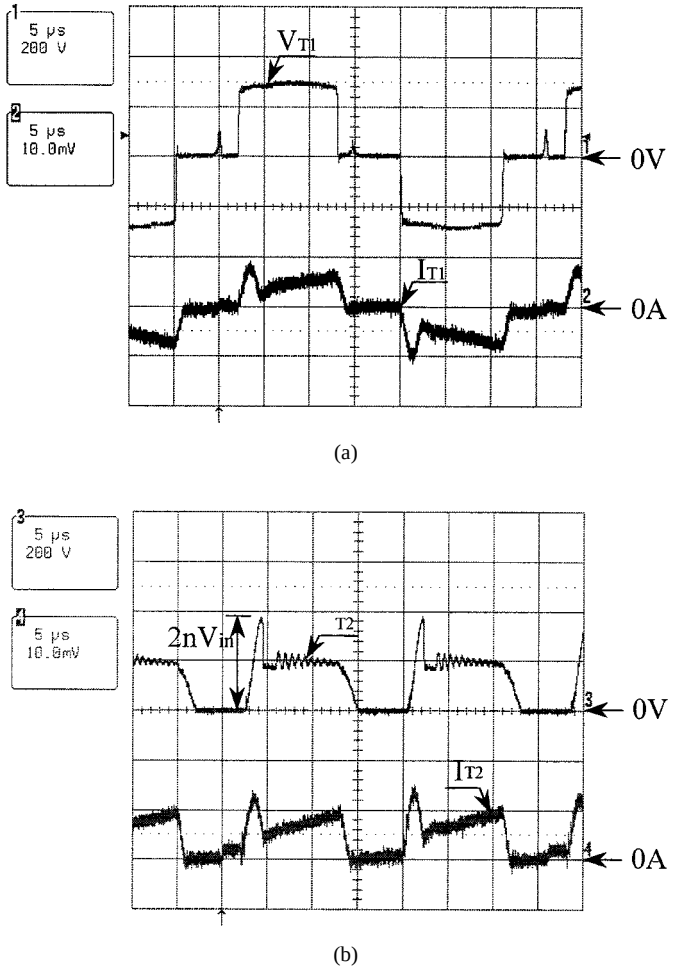

Fig. 9. Waveforms of ZVZCS FB dc/dc converter with ERS1 (200 V/div, 50 A/div, 5 μs/div). (a) Voltage and current waveforms of the primary. (b) Voltage and current waveforms of the secondary.

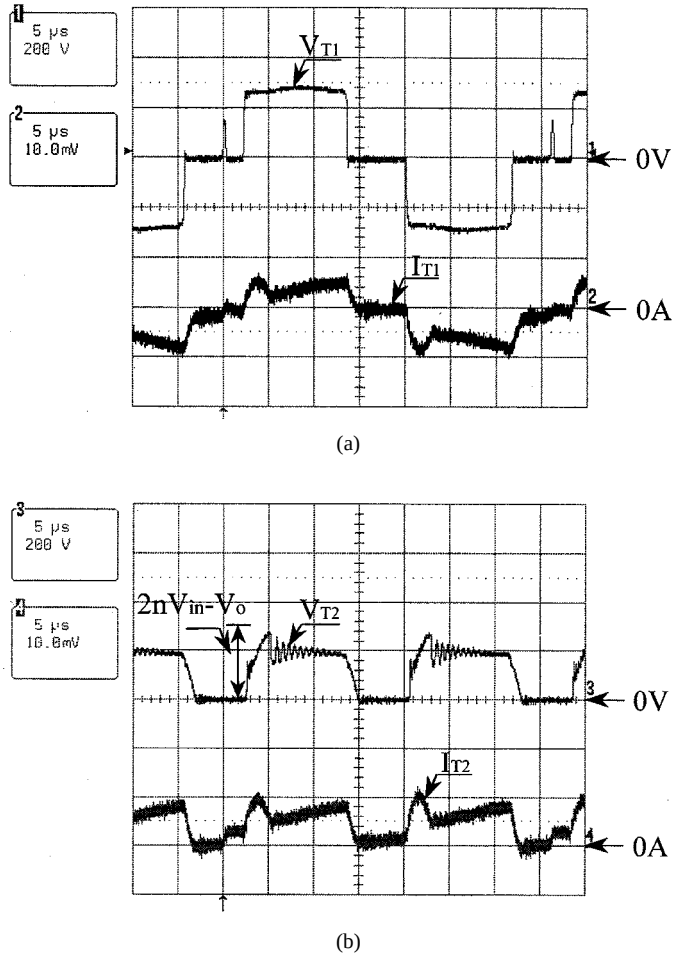

Fig. 10. Waveforms of ZVZCS FB dc/dc converter with the simplified energy-recovery snubber ERS2 (200 V/div, 50 A/div, 5 μs/div). (a) Voltage and current waveforms of the primary. (b) Voltage and current waveforms of the secondary.

regulator and the second term of ζ is the additional damping due to the effect of transformer leakage inductance and ERS. In the proposed ZVZCS FB dc/dc converter and the conventional ZVS FB dc/dc converter with the same transformer leakage inductance (L_l : 3.5 μH), the simulation results of the control-to-output voltage transfer functions for different load condition are shown in Fig. 6 by using the simulation program Mathcad. As shown in Fig. 6, even through the effect of damping R_d due to transformer leakage inductance shown in (17) was also observed in the control-to-output voltage transfer functions of the conventional ZVS FB dc/dc converter [4], the ZVS FB dc/dc converter with a small leakage inductance has the peaking in the control-to-output voltage transfer function due to the resonance of the output inductor and capacitor. However, the proposed ZVZCS FB dc/dc converter with the same small leakage inductance can reduce the peaking in a control-to-output voltage transfer function compared to the ZVS FB dc/dc converter because the use of the ERS provides the additional damping. In particular, the damping effect in the proposed ZVZCS FB dc/dc converter is more dominant in the light-load condition contrary to the ZVS FB dc/dc converter. From Figs. 6 and 7, it can be seen that the gain and phase of the experimental measurements agree with the simulation results closely. Therefore, this makes the system a first-order system below the two-pole system. Also, this makes design of the feedback compensator simpler.

The experimental results of the control-to-output voltage transfer function of the ZVS and ZVZCS FB dc/dc converter are implemented at 50% load condition (4Ω) by the use of impedance analyzer (HP4194A).

V. Experimental Results

A 7-kW (120 Vdc, 58 A) 30-kHz IGBT—based experimental circuit has been implemented to demonstrate the operation. The parameters of the circuit are as follows:

- Q_1–Q_4: IGBT (2MBI120L060, 600 V, 200 A);
- D_1–D_4: antiparallel diodes of IGBT;
- L_m : 286 μH (magnetizing inductance);
- L_l : 3.5 μH (leakage inductance of transformer);
- n: transformer turns ratio ($n = N_s/N_p = 6/8 = 0.75$);
- C_{s1}, C_{s2} : 0.2 μF (snubber capacitor);
- C_p: 14 nF (stray capacitance of IGBT);
- D_{s1}–D_{s4}: snubber diode;

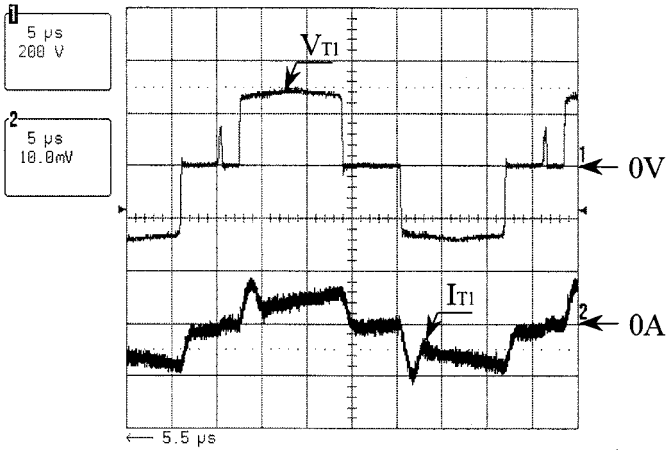

(a)

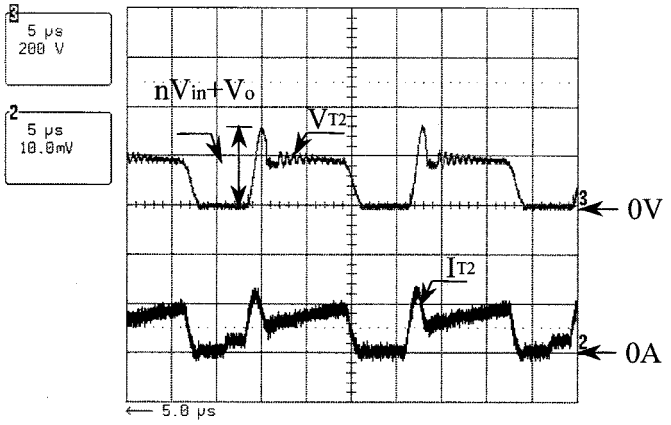

(b)

Fig. 11. Waveforms of the improved ZVZCS FB dc/dc converter with the modified energy-recovery sbubber ERS3 (200 V/div, 50 A/div, 5 μs/div). (a) Voltage and current waveforms of the primary. (b) Voltage and current waveforms of the secondary.

- D_5, D_6, D_7: 600 V, 100 A, t_{rr}: 150 ns (rectifier, freewheeling diode);
- L_f : 300 μH (output inductor, R_1 : 0.01 mΩ);
- C_o : 4700 μF (output capacitor, R_c : 1.08 mΩ);
- δt : 1.3 μs (dead time).

Figs. 8 and 9 show the voltage and current waveforms of the primary and secondary side of the transformer in the ZVS FB dc/dc converter with an *RCD* snubber and the ZVZCS FB dc/dc converter with the ERS (ERS1), respectively. Comparing Fig. 9 with Fig. 8, it can be seen that by using the ERS (ERS1), the circulating current in Fig. 9 decreases nearly to zero during the freewheeling interval and the converter achieves ZVS for the secondary rectifier diodes and the freewheeling diode. But, it can be seen that a transient overvoltage is produced in the secondary rectifier diodes of the converter. To reduce the transient overvoltage of the secondary and the circulating current, the ZVZCS FB dc/dc converter using the simplified ERS (ERS2) can be used. However, this converter, using the simplified snubber (ERS2), cannot achieve the ZVS in the secondary side as shown in Fig. 10(b). However, by using the modified ERS (ERS3), we can see that the converter can reduce the circulating current flowing through switching devices

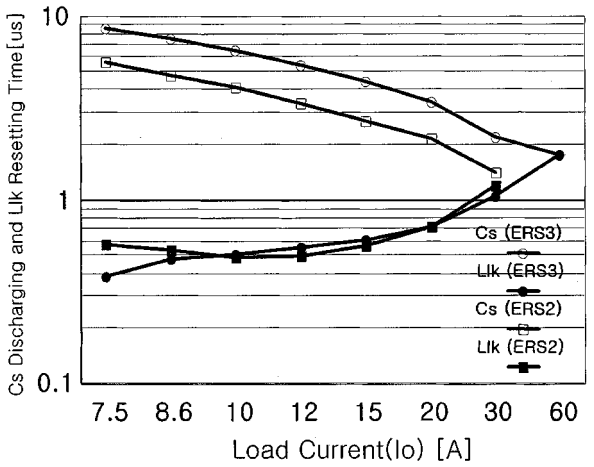

Fig. 12. Measurement results of C_s discharging time and L_{lk} resetting time in ZVZCS FB converters using ERS2 and ERS3.

during the freewheeling interval and reduce the voltage stress in the secondary rectifier diodes as shown in Fig. 11. Fig. 12 shows the operating characteristics of C_s discharging time and L_{lk} resetting time during the circulating interval in the ZVZCS FB converter using the simplified snubber (ERS2) and the modified snubber (ERS3), respectively. In the case of the ZVZCS FB converter using ERS1 or ERS3, the total capacity and capacitance of the snubber capacitor to reset the transformer leakage energy become double that of the ZVZCS FB converter using the simplified snubber (ERS2). Therefore, by using the proposed modified clamp circuit (ERS3), the ZVZCS condition can be expanded to the heavy load. The proposed converter has efficiency characteristics over 94% at full load (58 A).

VI. Conclusion

A ZVZCS FB dc/dc converter using the modified ERS was introduced in this paper. The proposed converter can reduce the secondary transient overvoltage as well as circulating current. Also, the design equations and model predictions were verified by simulation and experimental results. Because the ERS provides an additional damping, the proposed converter can reject the peaking due to the resonance of the output inductor and capacitor in a control-to-output voltage transfer function. Both analysis and experiment were performed to verify the proposed topology by implementing a 7-kW(120Vdc, 58 A) 30-kHz IGBT-based experimental circuit.

References

[1] S. Hamada, M. Michihira, and M. Nakaoka, "Using a tapped inductor for reducing conduction losses in a soft switching PWM DC-DC converter," in *Proc. EPE*, 1993, pp. 130–134.

[2] E. S. Kim, K. Y. Joe, M. H. Kye, Y. H. Kim, and B. D. Yoon, "An improved soft switching PWM FB DC/DC converter for reducing conduction losses," *IEEE Trans. Power Electron.*, vol. 14, pp. 258–264, Mar. 1999.

[3] J. C. Cho and J. W. Back *et al.*, "Novel zero-voltage and zero-current-switching (ZVZCS) full bridge PWM converter using a simple auxiliary circuit," in *Proc. IEEE APEC'98*, 1998, pp. 834–839.

[4] V. Vlatkovic, J. A. Sabate, R. B. Ridley, F. C. Lee, and B. H. Cho, "Small -signal analysis of phase-shifted PWM converter," *IEEE Trans. Power Electron.*, vol. 7, pp. 128–135, Jan. 1992.

Eun-Soo Kim (M'01) received the B.S., M.S., and Ph.D. degrees from Chung-Ang University, Seoul, Korea, in 1986, 1988, and 2000, respectively.

From 1989 to 2001, he was a Senior Researcher in the Power Electronics Research Division, Korea Electro-technology Research Institute (KERI). Since 2001, he has been an Assistant Professor in the Department of Electrical and Electronic Engineering, Jeonju University, Jeonju, Korea. His primary areas of research interest include soft-switching dc/dc converters, power-factor-correction circuits, and DSP applications.

Yoon-Ho Kim (M'88–SM'02) received the B.S. degree from Seoul National University, Seoul, Korea, the M.S. degree from the State University of New York, Buffalo, and the Ph.D. degree from Texas A&M University, College Station, all in electrical engineering.

He is currently a Professor in the Department of Electrical Engineering, Chung-Ang University, Seoul, Korea. His main interests are industrial electronics and drives.

Dr. Kim has been a Vice President of the Korean Institute of Power Electronics since 2001.